HHS Public Access

Author manuscript

Cutan Ocul Toxicol. Author manuscript; available in PMC 2016 November 03.

Published in final edited form as:

Cutan Ocul Toxicol. 2013 March ; 32(1): 18–22. doi:10.3109/15569527.2012.694090.

The effect of physiologic aqueous solutions on the perovskite material lead-lanthanum-zirconium titanate (PLZT)

William J. Foster,

Department of Physics, the University of Houston, Houston, TX, USA, Department of Ophthalmology, Weill-Cornell Medical College at the Methodist Hospital, Houston, TX, USA, The Methodist Hospital Research Institute, Houston, TX, USA

James K. Meen, and

Department of Chemistry and the Texas Center of Superconductivity at the University of Houston, Houston, TX, USA

Donald A. Fox

College of Optometry, Department of Biology and Biochemistry and Department of Pharmacology, the University of Houston, Houston, TX, USA

Abstract

Context—Perovskite compounds, including Lead-Lanthanum-Zirconium Titanate (PLZT), have wide technological application because of their unique physical properties. The use of PLZT in neuro-prosthetic systems, such as retinal implants, have been discussed in a number of publications. Since inorganic lead is a retinotoxic compound that produces retinal degeneration, the long-term stability of PLZT in aqueous biological solutions must be determined.

Objective—We evaluated the stability and effects of prolonged immersion of a PLZT-coated crystal in a buffered balanced salt solution.

Materials and Methods—Scanning Electron Microscopy and Electron Dispersive Spectroscopy (EDS) using a JEOL JSM 5410 microscope equipped with EDS were utilized to evaluate the samples before and after prolonged immersion.

Results—We found that lead and other constituents of PLZT leached into the surrounding aqueous medium.

Discussion—By comparing the unit cell of PLZT with that of $CaTiO_3$, which has been found to react with aqueous fluids, Lead is in the same site in PLZT as Ca is in $CaTiO_3$. It is thus reasonable that PLZT will react with aqueous solutions.

Conclusion—The results suggest that PLZT must either be coated with a protective layer or is not appropriate for long-term *in vivo* or *in vitro* biological applications.

DECLARATIONS OF INTEREST

The authors report no other declarations of interest.

INTRODUCTION

Perovskite compounds, including Lead-Lanthanum-Zirconium Titanate (PLZT), have wide technological application because of their unique physical properties. As a result of the non-uniform charge distribution within the unit cell of the crystal, these compounds have diverse properties including piezoelectricity and the anomalous ferroelectric photovoltaic effect (1, 2). When a crystal of PLZT is mechanically deformed, the positive and negative charge centers displace by differing amounts (3). Given the increasing interest in biomedical applications of advanced materials, perovskite compounds have been considered for use in different biological systems. All of these applications require that the compound is stable in aqueous biological solutions during both short-term and long-term use.

Perovskite compounds have been evaluated as possible components of biological assays for rapid clinical diagnostics (4, 5, 6). For these short-term assays, several studies determined that aqueous solutions do not etch or chemically modify the surfaces of mixed perovskite compounds (7, 8, 9, 10, 11, 12, 13). The use of perovskite compounds for advanced neuro-prosthetic systems, such as retinal implants have been discussed (14). Inorganic lead, a component of PLZT, is a retinotoxic compound that produces retinal degeneration (15, 16). In addition, aluminum (a common component of substrates used to grow PLZT crystals) and lanthanum have been implicated in structural and functional damage to the retina in mammalian eyes (17, 18, 19). Therefore, the long-term stability of PLZT in aqueous biological solutions must be determined. We evaluated the stability and effects of prolonged immersion of a PLZT-coated crystal in a buffered balanced salt solution.

METHODS

In order to investigate the effects of prolonged immersion of PLZT in a physiologic solution, we fabricated supported PLZT samples, immersed the substrates in a physiological salt solution, and analyzed the resulting samples using electron microscopy and spectroscopy.

PLZT was epitaxially grown on a single crystal $LaAlO_3$(012) substrate by pulsed-laser deposition, as described previously(20). Briefly, commercially purchased $LaAlO_3$ substrates were cleaned in acetone and methanol ultrasonic baths. The PLZT films were deposited at a temperature of 650°C in a 250 mTorr oxygen atmosphere using a 248 nm-KrF excimer laser with frequency of 5 Hz and laser fluence of 2–3 mJ/pulse for 20 minutes. Under these conditions, the resulting film thickness was 3000 nm. After deposition, the films were *in situ* annealed at 650°C, maintaining the O_2 pressure for 50 minutes, before cooling down to room temperature. No *ex situ* annealing was employed. The quality of the atomic order in the film was confirmed by x-ray diffraction (data not shown) and Scanning Electron Microscopy (SEM) measurements. The (100) direction (3) was found to be normal to the growth surface. All samples were stored in a desiccator until utilized.

Balanced Salt Solution Plus® was obtained from Alcon Laboratories and used without further modification. Each mL of the product contains: sodium chloride 7.14mg, potassium chloride 0.38 mg, calcium chloride 0.154 mg, magnesium chloride hexahydrate 0.2 mg, dibasic sodium phosphate 0.42 mg, sodium bicarbonate 2.1 mg, dextrose 0.92 mg, and

glutathione disulfide (oxidized glutathione) 0.184 mg. The reconstituted product had an adjusted pH of 7.40 ± 0.01 and an osmolarity of 305 ± 3 mOsm.

An Olympus BX-41 light microscope with UMPlanFI objectives was utilized to visualize all samples prior to electron microscopy. SEM and Electron Dispersive Spectroscopy (EDS) were performed utilizing a JEOL JSM 5410 microscope equipped with EDS. An accelerating voltage of 15 kV was used for all experiments. The substrates were not coated with a conducting metal because that would affect the results of subsequent immersion. Thus, the image quality was slightly limited by the insulating nature of the substrates. Data was segregated by sample and region measured (as characterized by SEM: particle, darker flat region, or lighter flat region) and these areas were statistically compared with pre-immersion data.

Electron diffraction was performed utilizing a JEOL JSM 6330F SEM and an Oxford Instruments OPAL System Electron Backscattering Diffraction System (EBDS). A 30 kV accelerating potential and 12 μamp current at the gun were used for EBDS. The sample was held at 70 degrees to the horizontal and the diffracted and backscattered electrons were collected on a phosphor screen, 25 mm in diameter and 25 mm from the target. The working distance was 15 mm. The material contributing to the diffraction pattern was in a region ~200 nm in diameter and ~50 nm in depth. Data were collected for 0.5–1 s at each point.

All studies were performed in quadruplicate and 15 areas were sampled on each substrate. The data were analyzed using one-way analysis of variance (ANOVA) with Scheffe post-hoc tests performed when appropriate. A paired t-test was performed on each sample, between each element prior to treatment, and each morphologically different area of the sample observed after treatment. A p value of < 0.05 was considered significantly different than controls.

RESULTS

Light microscopy revealed that samples immersed in the buffered balanced salt solution with glutathione for one month were decorated with profuse, grey, microscopic particles that were distributed almost uniformly across the sample. SEM also demonstrated profuse microscopic spheres, distributed almost uniformly across the sample that had been immersed in BSS with glutathione for one month (Figure 1).

EDS demonstrated a marked heterogeneity in the concentration of the various elements. The results for a characteristic sample area are displayed as a function of percent element (Figure 2). In all samples, there was a statistically significant change in the concentration of at least four elements after treatment (Table 1). The change and 95% confidence intervals for elements present in the pre-immersion sample is provided in Table 2. Electron Backscattered Diffraction (EBSD) demonstrated a uniform diffraction ring (Figure 3), consistent with an amorphous material.

DISCUSSION

In all samples, there was marked heterogeneity in the presence of the various elements and a statistically significant change in the concentration of at least four elements after treatment, demonstrating degradation of the samples by a physiological aqueous solution. The findings in this study can be explained if we consider the similarity of the unit cell of the perovskite material $CaTiO_3$ to PLZT. Calcium in $CaTiO_3$ is in the same location as lead is in PLZT. In $CaTiO_3$, the loss of calcium drives the reactivity with aqueous liquids (21). Increasing the concentration of calcium in the solution prevents dissolution of $CaTiO_3$ (22). It is then reasonable, as we found, for PLZT to leach lead into the surrounding solution. Thus, lead is selectively leached out of the near-surface layers, leaving a lead depleted surface. This finding is consistent with the $CaTiO_3$ model (23).

Given the changes in PLZT film stoichiometry after one-month immersion in aqueous solution, it cannot be considered an unreactive compound when immersed in aqueous solutions for biomedical applications. A number of elements, with known effects on biological systems, such as lead and other toxic divalent metals are released from PLZT. In addition, changes in the composition of the PLZT device will result in changes in device function and/or malfunction of the device. For this reason, piezoelectric materials (such as PLZT) must be protected from aqueous environments when utilized in such environments.

CONCLUSIONS

Our quantitative results describe changes in PLZT thin films immersed in aqueous solutions and demonstrate that, over time, devices fabricated with PLZT will release potentially toxic metal compounds into the aqueous solution and will slowly change their physical properties. For this reason, such devices must be protected from an aqueous environment or the potential interactions with the aqueous environment must be taken into account in the design of any device.

Acknowledgments

WJF was funded in part by the NEI and NIBIB of the NIH (EY017112 and EY007551), and the National Academies Keck Futures Grant in Advanced Prosthetics. DAF was funded in part by RO1 ES012482 and P30 EY07551.

REFERENCES

1. Brody PS. Large polarization dependent photovoltages in ceramic $BaTiO_3$ + 5 wt% $CaTiO_3$. Solid State Commun. 1973; 12:673–676.
2. Lin H, Wu NJ, Geiger F, Xie K, Ignatiev A. A ferroelectric-superconducting photodetector. J Appl Phys. 1996; 80:7130–7133.
3. Fridkin, VM. Springer Series in Solid State Science, vol. 9. New York, NY: Springer-Verlag; 1979. Photo-ferroelectrics; p. 85-86.
4. Guilbault GG, Jordan JM. Analytical uses of piezoelectric crystals: A review. CRC Crit Rev Anal Chem. 1988:19.
5. Andle, J.; Lec, RM. A monolithic piezoelectric sensor (MPS) for sensing chemical, biochemical and physical measurements. U.S. Patent. 6033852. 2000.

6. Kumar A. Biosensors based on piezoelectric crystal detectors: Theory and application. JOM-e. 2000; 52(10)
7. Veretnik D, Reich S. Structural and chemical stability in nonrandom silver-$YBa_2Cu_3O_7$ composites in the presence of water. Appl Phys Lett. 1990; 56:2150–2151.
8. Yokota K, Kura T, Ochi M, Katayama S. Degradation of high-temperature superconductor $YBa_2Cu_3O_{7-x}$ in water. Jpn J Appl Phys. 1990; 29:L1425–L1427.
9. Veretnik D, Mombru A, Reich S. Enhancement of crystallinity in $YBa_2Cu_3O_{7-x}$ ceramic by water or NaOH solution attack. Physica C. 1993; 209:191–194.
10. Rekhi S, Bhalla GL, Trigunayat GC. Recovery of superconductivity in the water degraded YBCO samples. Physica C. 1998; 307:51–60.
11. Jones, RE.; Schwartz, RW.; Summerfelt, SR.; Yoo, IK. Ferroelectric Thin Films VII. Symposium. Warrendale, PA: Mater Res Soc; 1999. The effect of atmospheric water vapour on the temperature dependence of capacitance in $Ba_xSr_{1-x}TiO_3$ thin films; p. 35
12. Fu, X.; Wang, D.; Yang, J. Proceedings of the 6th International Conference on Properties and Applications of Dielectric Materials. Piscataway, NJ: IEEE Press; 2000. The properties of water degraded superconducting $YBa_2Cu_3O_x$ film; p. 1006-1007.
13. Yu FC, Lin CH, Wang CM, Kao HCI. Kinetic study on the reaction of $YBa_2Cu_3O_y$ powder with water. Int J Mod Phys B. 2003; 17:3629–3635.
14. Zomorrodian, A.; Wu, NJ.; Wilczak, S.; Colbert, C.; Ignatiev, A.; Garcia, CA. La-doped $PbZrTiO_3$ thin film optical detectors for retinal implantation- A bionic eye. In: White, G.; Tsurumi, T., editors. ISAF. 2002. Proceedings of the 13th IEEE International Symposium on Applications of Ferroelectrics. New York, NY: IEEE; 2002. p. 129-132.
15. Fox DA, Campbell ML, Blocker YS. Functional alterations and apoptotic cell death in the retina following developmental or adult lead exposure. Neurotoxicology. 1997; 18:645–665. [PubMed: 9339814]
16. He L, Poblenz AT, Medrano CJ, Fox DA. Lead and calcium produce photoreceptor cell apoptosis by opening the mitochondrial permeability transition pore. J. Biol. Chem. 2000; 275:12175–12184. [PubMed: 10766853]
17. Lansdown AB. Metal ions affecting the skin and eyes. Met Ions Life Sci. 2011; 8:187–246. [PubMed: 21473382]
18. Lu ZY, Gong H, Amemiya T. Aluminum chloride induces retinal changes in the rat. Toxicol Sci. 2002; 66:253–260. [PubMed: 11896292]
19. Cervetto L, McNaughton PA. The effects of phosphodiesterase inhibitors and lanthanum ions on the light-sensitive current of toad retinal rods. J Physiol. 1986; 370:91–109. [PubMed: 2420982]
20. Zomorrodian A, Wu NJ, Song Y, Stahl S, Ignatiev A, Trexler EB, Garcia CA. Micro photo detector fabricated of ferroelectric-metal heterostructure. Jpn J Appl Phys. 2005; 44:6105–6108.
21. Zhang Z, Blackford MG. Aqueous dissolution of perovskite ($CaTiO_3$): Effects of surface damage and [Ca^{2+}] in the leachant. J Mater Res. 2005; 20:2462–2473.
22. Myhra, S.; Pham, DK.; Smart, RSC.; Turner, PS. Surface reactions and dissolution of ceramics and high temperature superconductors. In: Nowotny, J., editor. Science of Ceramic Interfaces. Amsterdam: Elsevier; 1991. p. 569-610.
23. Myhra S, Bishop HE, Riviere JC. Hydrothermal dissolution of perovskite ($CaTiO_3$). J Mater Sci. 1987; 22:3217–3226.

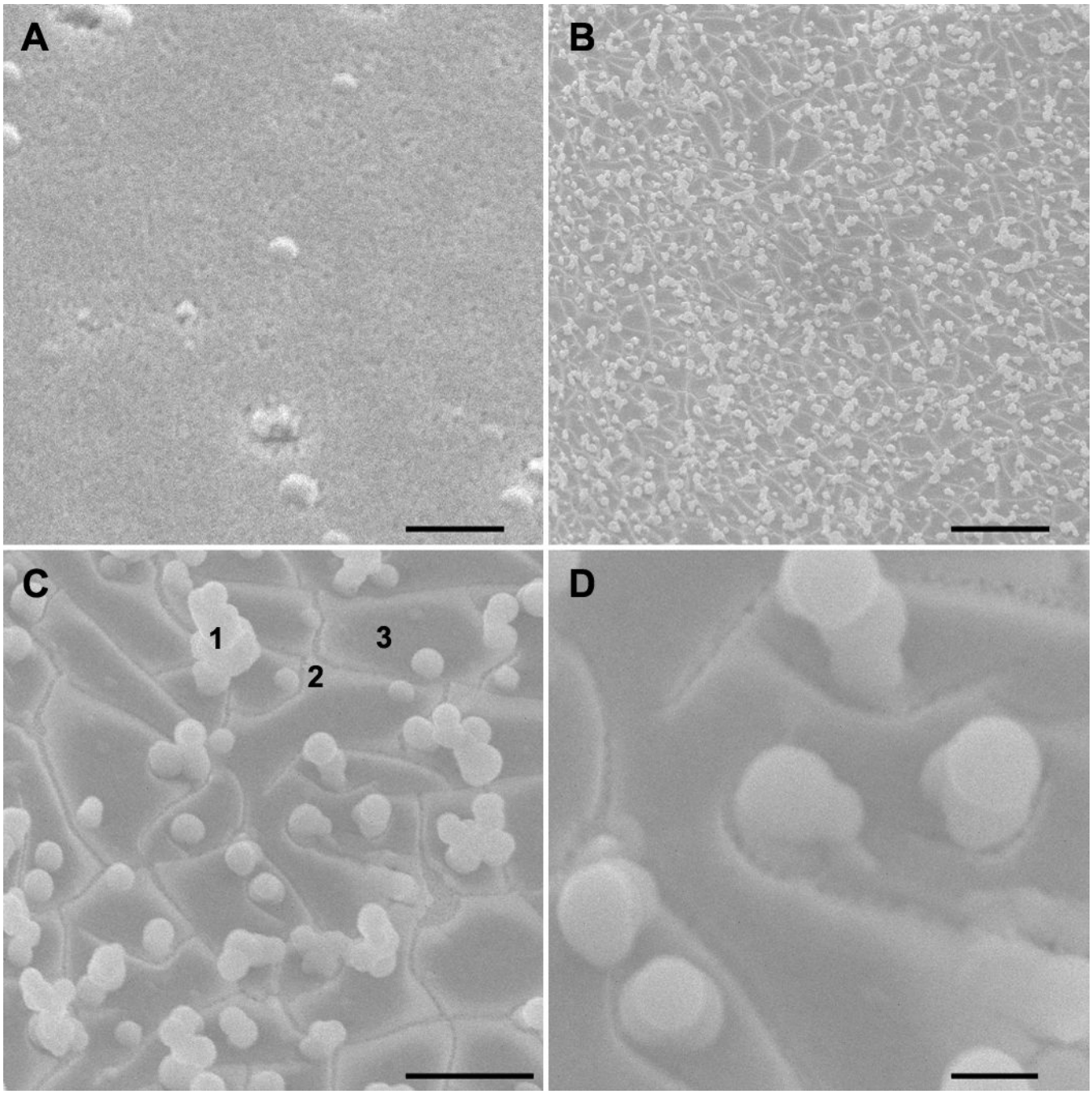

Figure 1.

SEM images of characteristic regions (upper left to lower right): before immersion (upper left) and after immersion for a month in BSS with glutathione solution (magnification 1k, 5k, 15k). Note the uniform particles and inhomogeneity of the surface. For analysis, the surface was divided into three domains: (1) particles, (2) light areas, and (3) dark areas. Scale bars 10 μm, 10 μm, 5 μm and 1 μm.

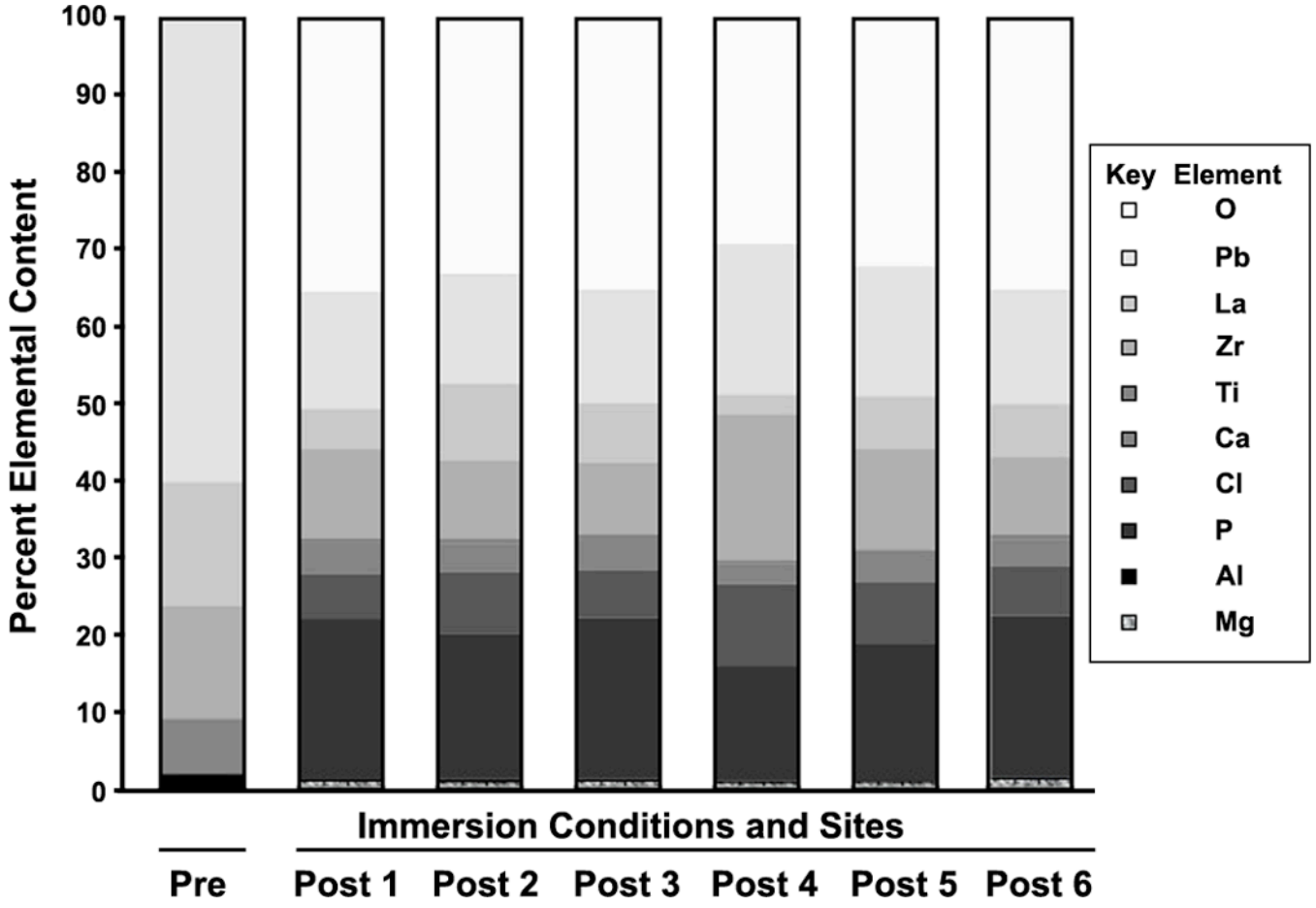

Figure 2. Representative example of EDS results

Pre-immersion data is represented by the left column, labeled 'Pre', while the remaining data is taken from particles on the sample after a month of immersion, with each separate particle labeled Post 1, Post 2, Post 3, etc. Consistent with the inhomogeneous surface appearance, the post-immersion sample composition is inhomogeneous, with less lead present on the surface after immersion. Similar data were also obtained from other domains (i.e. the light areas, for example) and analyzed to produce Table 1.

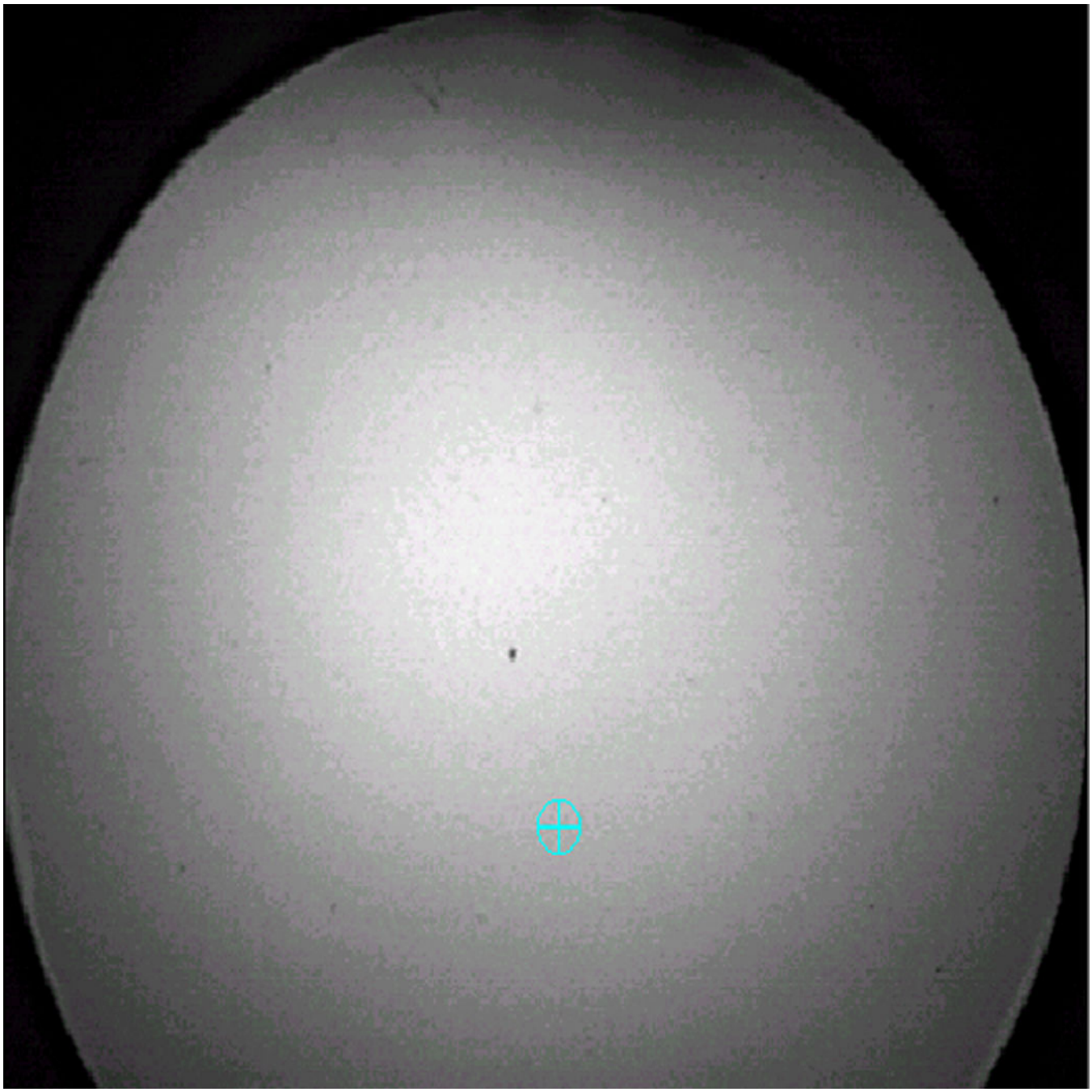

Figure 3. Characteristic Electron Backscattered Diffraction (EBSD) results on a particle
Note the ring structure, consistent with the diffraction pattern of an amorphous material.

Table 1

P-values for each element in the light areas following prolonged immersion in a buffered balanced salt solution

P-values describing the statistical significance in the content of each element, as determined by EDS, in the lighter flat regions of a sample after immersion. Each column corresponds to a different area on a characteristic sample. Note the inhomogeneity of the sample, even in visibly similar lighter areas, in that differences in at least four elements in each sample were statistically significant ($p < 0.05$, highlighted in grey) when compared with the sample prior to immersion.

Element	Samples								
	sample 1	sample 1	sample 2	sample 2	sample 2	sample 3	sample 3	sample 4	sample 4
Mg	0.1819	0.0029	0.0639	0.1024			0.0048	0.1169	0.1024
Al	0.0008	0.0009	0.0017	0.4069	0.0001	0.0006	0.0001	0.1169	0.4069
P	0.0008	0.001	0.0003	0.015	0.009				
Cl	0.391	0.009						0.0174	0.015
Ca	0.126	0.0005	0.0019	0.1034	0.0569	0.0021	0.003	0.0432	0.1034
Ti	0.0001	0.0001	0.0002	0.0005	0.0005	0.5194		0.0013	0.0005
Zr		0.0218	0.0001	0.4659	0.0002	0.0021	0.0035	0.2437	0.4659
La	0.0001	0.0246	0.0034	0.1493	0.0001			0.0166	0.1493
Pb	0.0696	0.0001	0.4907	0.004	0.0528	0.0005	0.0022	0.0046	0.004
O	0.0004	0.0004	0.0001	0.0008	0.0053	0.0001	0.0004	0.0002	0.0008

Table 2

Changes in elements after immersion

Mean, standard error of the mean, 95% confidence intervals, and significance (p-values) for the difference between the samples pre- and post-immersion. As shown in Figure 1, the samples have been divided into 3 domains for analysis (Light, Dark, and Particles).

Element	Difference between Means ± SEM (Pre vs Light)	95% C.I.	P value	Difference between Means ± SEM (Pre vs Dark)	95% C.I.	P value	Difference between Means ± SEM (Pre vs Particles)	95% C.I.	P value
Al	2.16 ± 0.60	0.91 to 3.41	0.002	3.80 ± 1.09	0.77 to 6.83	0.025	2.82 ± 1.44	−0.23 to 5.87	0.067
Ti	4.44 ± 0.79	2.72 to 6.15	<0.001	4.60 ± 1.64	0.04 to 9.15	0.049	4.49 ± 0.65	3.11 to 5.87	<0.001
Zr	−12.44 ± 4.88	−0.97 to 1.09	0.063				2.21 ± 4.52	−8.00 to 12.43	0.636
La	23.15 ± 8.13	3.26 to 43.05	0.029				20.50 ± 8.40	2.18 to 38.81	0.031
Pb	−3.063 ± 6.78	−18.16 to 12.03	0.661	17.42 ± 10.68	−10.04 to 44.88	0.164	30.24 ± 5.92	17.69 to 42.79	<0.001